Journal of Nanostructure in Chemistry (2018) 8:321–331
https://doi.org/10.1007/s40097-018-0276-3

ORIGINAL RESEARCH

Influence of calcination temperature on the activity of mesoporous CaO/TiO_2–ZrO_2 catalyst in the esterification reaction

Aliakbar Sistani[1] · Naser Saghatoleslami[1,2] · Hamed Nayebzadeh[1]

Received: 15 June 2018 / Accepted: 9 August 2018 / Published online: 16 August 2018
© The Author(s) 2018

Abstract

In the present study, the effect of calcination temperature on the structure and performance of mesoporous CaO/TiO_2–ZrO_2 catalyst fabricated by sol–gel method used in the esterification reaction was assessed. Then, CaO/TiO_2 catalyst was also synthesized via the same method to evaluate the effect of zirconia cations on its properties and activity. The samples were characterized by X-ray Diffraction (XRD), Fourier transmittance infra-red (FT-IR), Brunauer–Emmett–Teller (BET)–Barrett-Joyner-Halenda (BJH), scanning electron microscope (SEM) and transmission electron microscopy (TEM) analyses. Moreover, Hammett indicator method was utilized to assess the acidity and basicity of the samples. It was found that zirconium was clearly incorporated in CaO/TiO_2 lattice and transformed that from amorphous phase to crystalline structure. In addition, the basicity and acidity of CaO/TiO_2 was clearly increased by zirconia loading. Evaluation of the samples' activity presented that CaO/TiO_2 catalyst exhibit no activity in the esterification reaction, while all CaO/TiO_2–ZrO_2 catalysts showed high ability to convert oleic acid to its ester. Moreover, the catalyst calcined at 400 °C showed the highest activity in the esterification reaction with desirable properties such as high crystallinity, acidity, basicity and surface area along with well-distribution of particle size and pore size. The best catalyst converted around 90% of oleic acid to ester at optimized conditions of 150 °C, 12:1 molar ratio of methanol/oleic acid, 3 wt% of catalyst for 4 h of reaction time. Moreover, the sample was successfully used for five runs without significant reduction in activity that makes it a suitable choice as a catalyst for industrial applications.

Graphical abstract

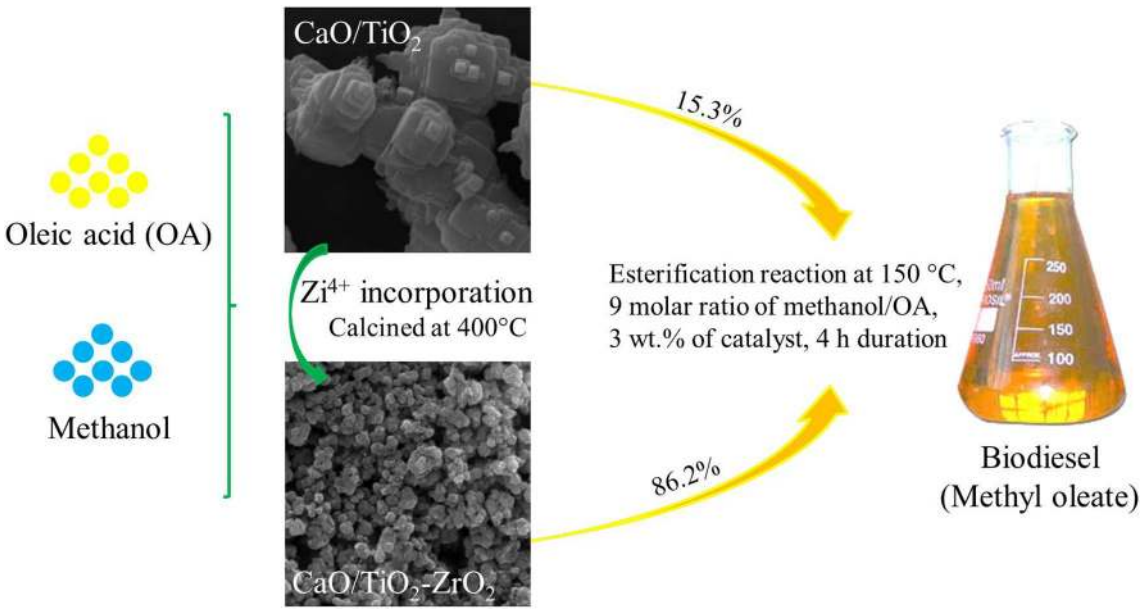

Extended author information available on the last page of the article

Keywords Heterogeneous catalyst · Zirconia · Titania · Calcination temperature · Sol–gel method, esterification

Introduction

Energy and environmental issues push the governments to allocate a lot of research funding to search for alternative fuels. Biomass-derived fuels such as methane, ethanol, and especially biodiesel are well-accepted alternatives. Among them, the properties of biodiesel are similar to those of fossil fuels which can be utilized in the engine with less modification. Biodiesel is composed of fatty acid methyl esters (FAMEs) and is usually produced via the transesterification of plant oils or animal fats with low molecular weight alcohols in the presence of a catalyst. To economically produce biodiesel, low cost oils such as waste cooking oil, and inedible oils must be utilized to reduce the biodiesel production cost [1, 2]. However, these oils contain a high amount of free fatty acids (FFAs) which react with homogeneous catalysts such as NaOH and KOH to form soap, which can reduce yield, increase the purification and neutralization steps and produce large amounts of waste water [3, 4]. Therefore, FFAs must be eliminated or converted before transesterification where the homogeneous acid catalysts such as H_2SO_4 are utilized for conversion of these materials to biodiesel (ester). However, the drawbacks of acid catalysts such as requirement of high reaction temperature and time, corrosion and acidic waste water persuade the researches to utilize heterogeneous catalysts instead of homogeneous catalyst [5, 6].

Due to some attractive properties of heterogeneous catalysts such as its easily recoverability, reusability, and noncorrosivity, various kinds of them have been developed in the last decades. These catalysts are classified in the basic and acidic classes, which can participate simultaneously in the esterification and transesterification reactions [7, 8]. Each of acidic and basic heterogeneous catalysts was used, so that titanium dioxide (TiO_2) and zirconium dioxide (ZrO_2) single oxides exhibit excellent catalytic properties as support or modifier. ZrO_2 is well-known in heterogeneous catalysts due to its chemical and thermal stability and simultaneous presence of both acidic and basic surface sites [9, 10]. TiO_2 is unique for its photo-catalytic and strong metal support interaction properties [11, 12]. Moreover, the alkaline earth metal oxides were extremely assessed for active site in the surface of base catalysts. Calcium oxide is well-known for biodiesel production due to its low price, high basic strength and good catalytic performance. However, leaching of Ca^{2+} ions from catalyst's surface into reaction media and easy deactivation by H_2O or CO_2 are its two major drawbacks [13–15].

Kawashima et al. [16] investigated thirteen different calcium-containing catalysts and reported that $CaTiO_3$, $CaMnO_3$, $Ca_2Fe_2O_5$, $CaZrO_3$, and $CaO–CeO_2$ showed high activities in the transesterification reaction. It was found that $CaZrO_3$ shows high durability and has the potential to be used in biodiesel production processes as heterogeneous base catalyst. Xia et al. [17] studied on the preparation of $CaO–ZrO_2$ via combustion method with various amounts of urea as fuel. They reported that formation of $CaZrO_3$ can increase the activity of esterification reaction rate by raising the strength of basic sites. The same result was obtained by Liu et al. [18] when the birch template method was utilized for fabrication of Ca/Zr mixed metal oxide and the yield of 92.6% was obtained at catalyst mass fraction of 8%, 72:1 M ratio of methanol to rapeseed oil, reaction temperature 120 °C and a reaction time of 6 h.

Mesoporous propyl sulfonic acid supported on TiO_2 was also examined in the transesterification reaction and 98.3% of FAME was obtained after 9 h of reaction time with 1:15 molar ratio of oil to methanol, 60 °C reaction temperature and 4.5 wt% catalyst loading [19]. Gardy et al. [20] fabricated magnetic $SO_4/Fe–Al–TiO_2$ to transesterified waste cooking oil. The anatase structure of TiO_2 was used as support and achieved 96% yield after 2.5 h of reaction at 90 °C, using 3 wt% of the magnetic catalyst, and a methanol:oil molar ratio of 10:1. Kesic et al. [21] evaluated the catalytic activity of $CaTiO_3$ as heterogeneous base catalysts. Although, they reported high stability of this catalyst for methanolysis of sunflower oil, no catalytic activity was observed at 60 °C. However, FAME yield of 90% was reached after 2 h at 165 °C. Furuta et al. [22] only examined the activity of amorphous zirconia solid catalysts supported by TiO_2 and Al_2O_3. They reported that titanium-doped amorphous zirconia is a promising catalyst for production of biodiesel fuels due to amphoteric nature of zirconia and high activity in both transesterification and esterification reaction.

Based on the results of studies, titanium cations can increase the stability of the catalyst and zirconia can accelerate the activity of the sample. However, according to our best knowledge, the use of calcium oxide/titania–zirconia as a mixed metal oxide for the esterification reaction has not yet been studied.

In this study, the production of biodiesel (ester) from esterification of oleic acid as FFA using CaO/TiO_2 supported/incorporated by zirconia as a heterogeneous nanocatalyst was investigated. The catalyst was prepared by a citrate sol–gel method and the effect of calcination temperature on its physicochemical properties was assessed. Finally, the reaction conditions such as reaction temperature, reaction time, methanol/oleic acid molar ratio and catalyst amount were optimized using the sample calcined at desirable temperature and the reusability was assessed.

Experimental

Materials

Zirconyl nitrate anhydrous ($ZrO(NO_3)_2{\cdot}xH_2O$, 99%, Sigma-Aldrich), calcium nitrate tetrahydrate ($CaN_2O_6{\cdot}4\,H_2O$, 99%, Merck) and titanium dioxide (TiO_2, 98%, Merck) were used as Zr, Ca and Ti precursors without further purification, respectively. Meanwhile, methanol, ethanol, oleic acid, citric acid and nitric acid synthesized in Merck co. were purchased from local supplier.

Catalyst preparation

$CaO/TiO_2–ZrO_2$ catalyst was synthesized by modified sol–gel method where citric acid was used as complex agent. For this purpose, 0.8 g TiO_2 was first dissolved in 30 ml of 14 M HNO_3 solution. In another beaker, 0.472 g calcium nitrate and 0.231 g zirconyl nitrate were homogeneously mixed in a small quantity of deionized water. Finally, the mixtures were added to each other and were mixed vigorously for approximately 20 min. Afterwards, citric acid was slowly added to the metal nitrate solution under constant stirring to control pH around 3. The solution was refluxed at 80 °C for 1 h and poured in the beaker and was subsequently heated for 30 min at 60 °C to remove excess water and become a highly viscous gel. The obtained gel was dried overnight in an oven at 110 °C and calcined at different temperatures in the range of 100–500 °C for 4 h. The samples were labeled as CTZ-100, CTZ-200, CTZ-300, CTZ-400, CTZ-500, respectively (see Fig. 1). The CaO/TiO_2 catalyst calcined at 400 °C (CT-400) was also synthesized with same procedure without adding zirconia precursor and labeled as CT-400.

Catalyst characterization

The crystalline phases of the samples were identified by XRD (UNISANTIS/XMD 300) using Cu K_α radiation ($\lambda = 1.5406$ Å) over 2θ range of 20°–80°. Moreover, the crystalline size of the samples was determined by Scherer's equation. FT-IR spectrum (Thermo Nicolet-AVATAR 370) in the range of 400–4000 cm^{-1} was used to determine the surface functional groups of catalysts. The specific surface area, mesoporous volume and mean pore size were determined by N_2 adsorption–desorption at − 196 °C using Belsorp mini II (BelJapan) system by the BET–BJH methods. Before analyzing, the samples were heated at 80 °C overnight to degas the porosities. SEM (LEO 1450 VP) and TEM (LEO 912AB) were utilized for assessment of the morphology and dimension of the samples. The acidic and basic properties of the samples were determined by mixing 300 mg of the each sample with 1 mL of a solution containing Bromothymol blue ($H_- = 7.2$), phenolphthalein ($H_- = 9.8$), and 2,4-dinitroaniline ($H_- = 15.0$) as basic indicators and methyl red ($H_0 = 4.8$), methyl orange ($H_0 = +3.3$) and violet crystal ($H_0 = 0.8$) as acidic indicators diluted in 10 mL of methanol as seen in the Hammett indicators method. The mixture was left for 2 h until no further color changes were observed. The acidic or basic strengths are quoted as being stronger than the weakest indicator that exhibits a color change, but weaker than the strongest indicator that produces no color change. Finally, benzene carboxylic and n-butylamine solutions were used to measure basicity and acidity of the samples, respectively [9, 23].

Catalyst testing

The esterification reaction was carried out for assessment of the catalytic activity of samples at 150 ± 2 °C for 4 h in constant stirring speed at 600 rpm. In each run, 10 g of oleic acid, 0.3 g of catalyst and 13 mL methanol (9 molar ratios to feedstock) were poured into 100 cm^3 stainless steel reactor equipped by thermocouple (Type K) and manometer. After the reaction, the reactor was cooled to room temperature and the mixture phases including ester, water and catalyst layers were separated using centrifuging (Sahand Universal co., Iran) at 2500 rpm for 20 min. Finally, pure biodiesel was obtained by heating the upper layer to remove excess methanol and water via heating at 90 °C for 2 h. The conversion was calculated by reduction of acidity index of oleic acid compared to its ester using titration with potassium hydroxide (0.1 M) as shown in the following equation [24].

$$\text{Conversion}\ (\%) = 100\left(\text{AV}_{\text{oleic acid}} - \text{AV}_{\text{methyl ester}}\right) / \text{AV}_{\text{oleic acid}}. \quad (1)$$

The acid value (AV) of the sample was obtained according to the suggested procedure. First, 0.5 g of sample was mixed with 50 mL methanol and two drops of phenolphthalein solution as indicator was added. The mixture was titrated with a solution of potassium hydroxide (0.1 M) to change the mixture color from colorless to purple. The AV was calculated as follows [25]:

$$\text{AV} = \frac{56.11 \times V \times N}{W}, \quad (2)$$

where V is mL of standard potassium hydroxide solution, N is normality of the potassium hydroxide solution and W is weight in g of sample.

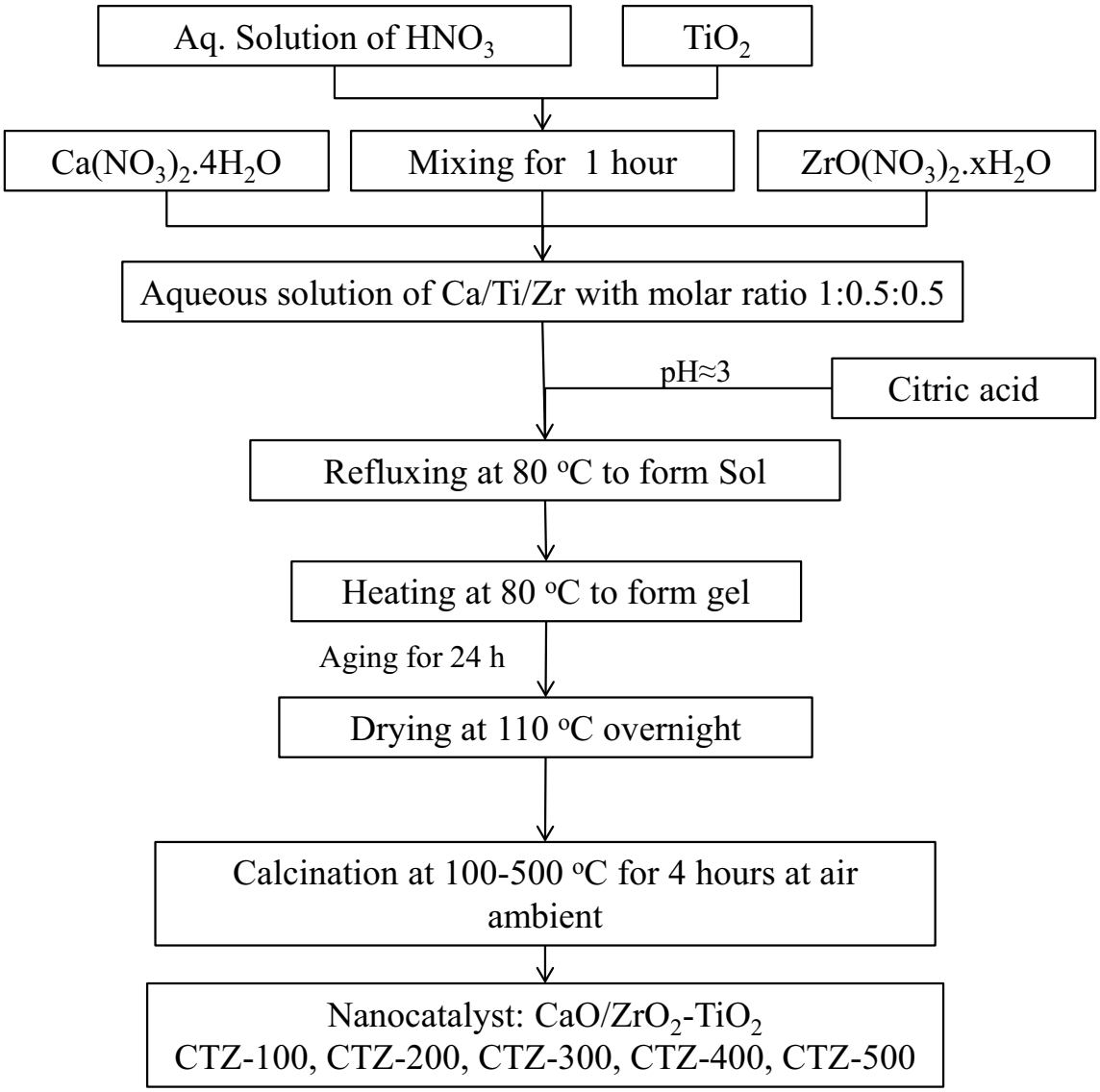

Fig. 1 Flowchart of preparation of $CaO/TiO_2–ZrO_2$ nanocatalyst

Results and discussion

Effect of calcination temperature on the performance and properties of CTZ

The researchers have reported that the calcination temperature largely affects the structure and catalytic properties of the resultant catalysts [26–28]. The temperature in the range of 300–600 °C was usually suggested as optimum for supported catalyst used in the biodiesel production process [29, 30]. The nanocatalyst calcined at different temperatures (100–500 °C) was tested in the esterification reaction to evaluate the effect of calcination temperature on the activity of fabricated catalyst. The results are illustrated in Fig. 2 and the sample calcined at 400 °C (CTZ-400) shows the highest catalytic activity that converted 86.2% of oleic acid to ester. The conversion enhanced from 60.6 to 86.2% by increasing the calcination temperature from 100 to 500 °C. By raising the calcination temperature more, the activity was reduced that can be found in the structural changes.

The CT-400 catalyst converted 15.3% of oleic acid to biodiesel at the same conditions that is much lower than CTZ-100 catalyst. It can prove the effect of zirconia as support for increasing the activity of a catalyst even at low calcination temperature.

XRD analysis

The XRD patterns of the samples are presented in Fig. 3. Figure 3a shows CT-400 catalyst with an amorphous

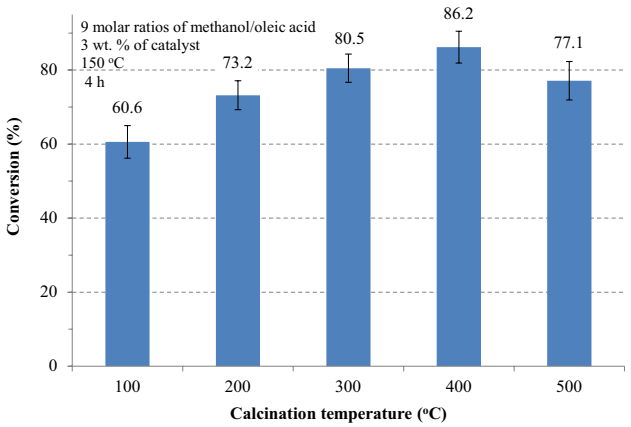

Fig. 2 The activity of $CaO/TiO_2–ZrO_2$ nanocatalyst calcined at different temperatures in the esterification reaction

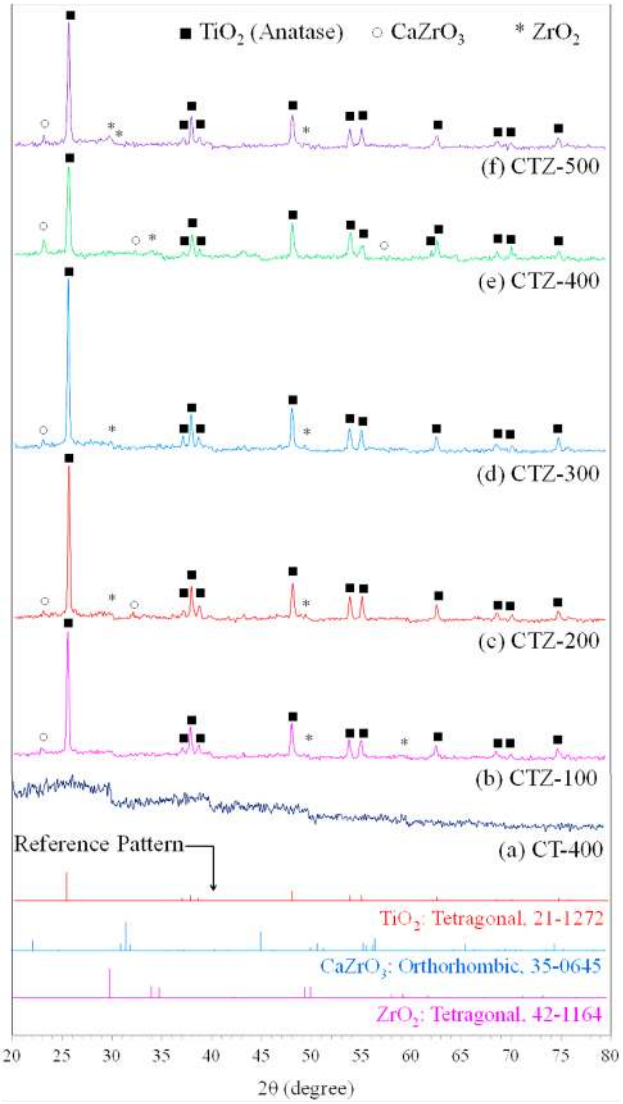

Fig. 3 XRD patterns of **a** CaO/TiO_2 nanocatalyst calcined at 400 °C and $CaO/TiO_2–ZrO_2$ nanocatalysts calcined at **b** 100, **c** 200, **d** 300, **e** 400 and **f** 500 °C

structure. Atitar et al. [31] reported that TiO_2 calcined at 500 °C showed the highest anatase phase and the sample calcined at temperature lower 400 °C had less crystallinity along with amorphous structure. However, when zirconia was loaded on CaO/TiO_2 catalyst it caused titanium oxide to transform from amorphous to crystalline form that was observed for all the samples calcined at different temperatures. The effect of zirconia on the reduction in the calcination temperature for formation of titania phases can be proved. Li et al. [32] presented that ZrO_2 can diffuse in the TiO_2 matrix and no diffraction of zirconia was observed. Moreover, they reported the anatase phases of TiO_2 were detected by doping the zirconium cations in the titania lattice.

The crystalline structure of anatase phase of titania (JCPDS no. 21–1272) is clearly observed for all $CaO/ZrO_2–TiO_2$ nanocatalysts at $2\theta = 25.3$, 37, 37.8, 38.6, 48.1, 54, 55.1, 62.1, 62.8, 68.8, 70.3, 74.2, 75.1 and 76.1° related to [101], [103], [004], [112], [200], [105], [211], [213], [204], [116], [220], [107], [215] and [301] crystallography, respectively [26, 33]. Some characteristic diffraction peaks of monoclinic and tetragonal phases of zirconia can be detected whereas these structures disappeared in CTZ-400 sample (Fig. 3e). This corresponded to high incorporation of ZrO_2 in CaO and/or TiO_2 lattice to form $CaZrO_3$ (JCPDS no. 35-0645), or $ZrTiO_4$ (JCPDS no. 34-0415) [34].

However, peaks of zirconia phases again appeared in CTZ-500 catalyst due to reduction of the interaction between zirconia and titanium at higher temperature which resulted in a decrease in the catalytic activity of CTZ-500 in comparison with CTZ-400, which is in consistency with other researches [27, 32, 35]. Mongkolbovornkij et al. [36] investigated the activity of zirconia modified by titania in the esterification of palm fatty acid distillate and reported that the phase of $TiO_2–ZrO_2$ was transformed from amorphous to crystalline phase above 500 °C. The results indicated that the citrate sol–gel method has high ability to synthesize the catalysts with high crystallinity and activity even in low temperature in spite of other catalyst preparation methods.

The crystallite size of the samples estimated by Scherer's equation at $2\theta = 25.5°$ and their relative crystallinity are listed in Table 1. The crystalline size of samples increased from 31.4 nm for CTZ-100 and CTZ-200 to 34.6 nm for CTZ-300 and then sharply decreased to 21 nm for CTZ-400. It was reported that zirconia has greater crystal size than those for titania. Therefore, the crystal size by rising the temperature was increased due to formation of more crystal form of titania and zirconia [31, 32]. However, due to well-perching of zirconia in the titania lattice and no formation

Table 1 Physicochemical properties of the samples

Nanocatalyst	Acidity		Basicity		Relative crystallinity[a]	Crystallite size[b] (nm)
	H_0	Strength (mmol/g)	H_-	Strength (mmol/g)		
CT-400	0.8–3.3	0.036	7.2–9.8	0.135	–	–
CTZ-100	0.8–3.3	0.253	7.2–9.8	0.225	82.8	31.4
CTZ-200	0.8–3.3	0.321	7.2–9.8	0.286	87.4	31.4
CTZ-300	0.8–3.3	0.379	7.2–9.8	0.313	100	34.6
CTZ-400	0.8–3.3	0.402	7.2–9.8	0.321	48.5	21.0
CTZ-500	0.8–3.3	0.371	7.2–9.8	0.318	78.9	32.9

[a]Relative crystallinity: XRD relative peak intensity at $2\theta = 25.5°$

[b]Crystallite size estimated by Scherre's equation at $2\theta = 25.5°$

of individual crystal of zirconia, the crystalline size was sharply reduced. Formation of zirconia phases resulted in increase of the crystalline size and CTZ-500 presented a greater crystalline size compared to CTZ-400 [34]. The same phenomenon was observed for the relative crystallinity where the relative crystallinity was increased by increasing the calcination temperature due to creation of appropriate medium to grow the crystals. However, the intensity of titania was clearly decreased when the sample was calcined at 400 °C because of incorporation of zirconia in the titania lattice.

Hammett indicators analysis

To evaluate the acidic and basic strengths of the sample, they were characterized by Hammett indicators. For example, it is well-known that the amount of acid on a solid is usually expressed as the number or mmol of acid sites per unit weight or per unit surface area of the solid. Two main methods are usually utilized for the determination of strength and amount of a solid acid including an amine titration method (*n*-butylamine titration) using Hammett indicators and a gaseous base adsorption method (ammonia and pyridine adsorption). In the amine titration method using indicators, the color of suitable indicators adsorbed on the surface will give a measure of its acid strength. If the color is that of the acid form of the indicator, then the value of the H_0 function of the solid is equal to or lower than the pKa of the conjugate acid of the indicator. The amount of acid sites on a solid surface can be measured by amine titration immediately after determination of acid strength by the above given method such that a solid acid suspended in benzene is titrated with *n*-butylamine, using an indicator. This method gives the sum of the amounts of both Bronsted and Lewis acid [37]. The same method with different indicators and titration solution, as described in the catalyst characterization section, was used for measuring the base strength of the samples. The results are presented in Table 1. It is observed that CT-400 exhibited the lowest acidity and basicity strength while these were significantly increased by addition of zirconia. This is because of two reasons: (1) the catalyst transforming from amorphous to crystal form and (2) amphoteric properties of zirconia. Formation of strong interaction between Ti^{4+} and Zr^{4+} and incorporation of Zr cations in calcium oxide lattice caused the acidic and basic strength of a catalyst to increase significantly [31, 35]. It is known that the activity of the catalysts may be strongly affected by the strength of base and acid together. By increasing the calcination temperature to 400 °C, basic and acidic strength are also get increased while further rising calcination temperature to 500 °C results in decrease in basic and acidic strength, which is in good agreement with other findings [30, 38]. It can be related to reduction in the bonding between Ti and Zr cations and the growth of titania crystals that reduced the interaction between solid acid surface and Hammett indicators solutions.

FT-IR analysis

The FT-IR spectra of catalysts calcined at various temperatures are shown in Fig. 4. It was reported that the Ti–O bonds can be observed in the range of 500–750 cm^{-1} while a broad peak (400–900 cm^{-1}) appeared in the samples. Li et al. [39] reported that the broad absorption peaks below 900 cm^{-1} in Zr/Ti mixed metal oxide structure can be assigned to Ti–O and Zr–O stretching vibrations. The weak peaks at 920 and 1080 cm^{-1} can be corresponding to stretching vibration bonds of Zr–O and Zr=O, respectively [9, 40]. The weak band at 1100–1200 cm^{-1} represents M–OH deformation (where M represents Ca, Zr or Ti metal ions) [41]. With increasing calcination temperature up to 400 °C, the peaks at 1300–1400 cm^{-1} which were assigned to the asymmetric and strong stretching vibrations of NO_3 ions disappeared, providing additional evidence for transformation of the sample from amorphous to crystal form and higher activity of calcined catalysts over 300 °C. The band that appeared at 1420 cm^{-1} is attributed to the carbonate groups due to adsorption of CO_2 on the catalyst surface [42]. The peak at 1600–1680 cm^{-1} belongs to (–C=O) stretching vibration

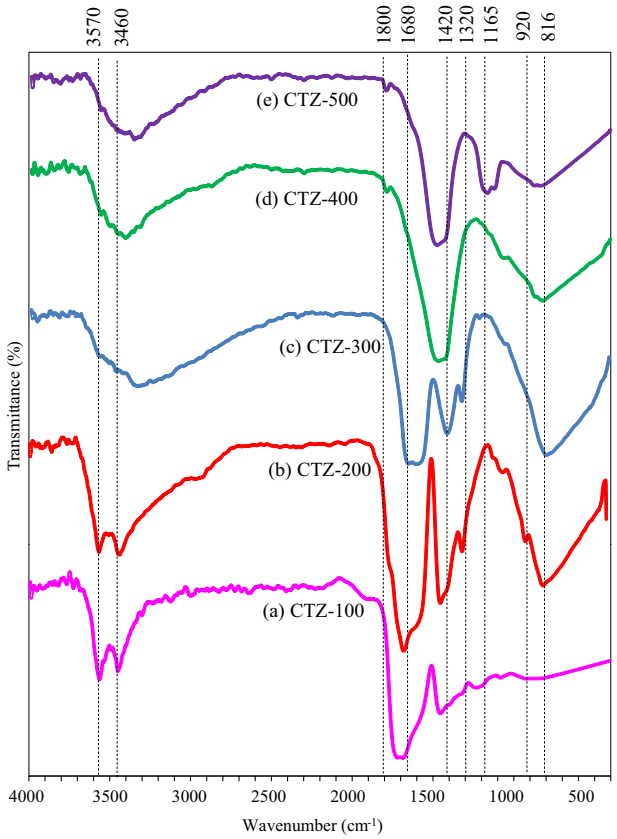

Fig. 4 FT-IR spectra of **a** CaO/TiO_2 nanocatalyst calcined at 400 °C and CaO/TiO_2–ZrO_2 nanocatalysts calcined at **b** 100, **c** 200, **d** 300, **e** 400 and **f** 500 °C

from citric acid and also may be bending vibration of H_2O molecules which overlapped and cannot be observed with increasing calcination temperature. The presence of broad bands around 3400–3600 cm^{-1} is related to the symmetric and asymmetric stretching of O–H that occur owing to the reaction between air moisture and surface of catalysts and/or metal ions with OH groups such as Ca–OH [43].

SEM and TEM analyses

To evaluate the effect of calcination temperature on the growth of particle and transformation of metal oxides from amorphous to crystal form, CTZ-100 and CTZ-400 nanocatalysts were characterized by SEM analysis. The SEM images are presented in Fig. 5. It could be obviously observed that calcination of the sample at higher temperature made significant changes in the surface and crystalline shape and size of the catalyst. CTZ-400 has uniform particle in comparison with CTZ-100 along with large external pores, which caused well permeation of large molecules of reactants to internal surfaces. Moreover, the particles shape of CTZ-400 nanocatalyst is closed to spherical form, while CTZ-100 showed a bulky and layered structure, which is related to lack of calcination treatment.

The TEM analysis of CTZ-400 was done to obtain its particle size and shape, accurately (Fig. 5c). The CTZ-400 catalyst exhibited relatively uniform particle with hexagonal shape. The average particle size of CTZ-400 is lower than 100 nm that can be classified in the nanoscale materials. In addition, each grain can be considered as a single crystallite that caused an increase in the surface area that lead to an increase in the interaction between reactants and catalyst surface.

BET and BJH analysis of CTZ-400 as the best catalyst

The textural properties of CTZ-400 as optimum nanocatalyst such as BET surface area, mean pore size and pore volume were, respectively, obtained as 274.5 m^2/g, 4.8 nm and 0.826 cc/g. It is noteworthy that the sample possessed pore diameters greater than 2 nm revealing that it is mesoporous material. The prepared nanocatalyst has very high surface area, and two ways were proposed for influence of a higher surface area on the catalytic activity: (a) formation of the highly dispersed active phase; and (b) easy accessibility of the reactants to surfaces [44].

The nitrogen adsorption–desorption isotherms and pore size distribution of the as-synthesized sample are presented in Fig. 6a. The nanocatalyst presented characteristic type IV curves with hysteresis loop of H1 type, which is related to cylindrical and spherical pores [45]. The pore size distribution of CTZ-400 nanocatalyst is shown in Fig. 6b. The wide range of pore size observed from the figure, especially the pores greater than 3 nm has significant volume. It was suggested that the porosity of the nanocatalyst must be greater than 3 nm for fast permeation of reactants into porosity and overcoming the diffusion problems [43, 46].

Optimization of the esterification reaction conditions

The effect of reaction parameters in the esterification reaction was examined using CTZ-400 as optimum nanocatalyst. The optimization results of reaction conditions including reaction temperature, reaction time, methanol/oleic acid molar ratio and catalyst loading are summarized in Table 2. The results showed that the conversion continuously increased from 40.3 to 87.5% by rising the reaction temperature from 90 to 180 °C. It is a fact that the esterification reaction is endothermic and a higher conversion will be reached when higher temperatures are used [47]. However, insignificant increase in the reaction conversion was observed when the temperature raised over 150 °C. Therefore, due to

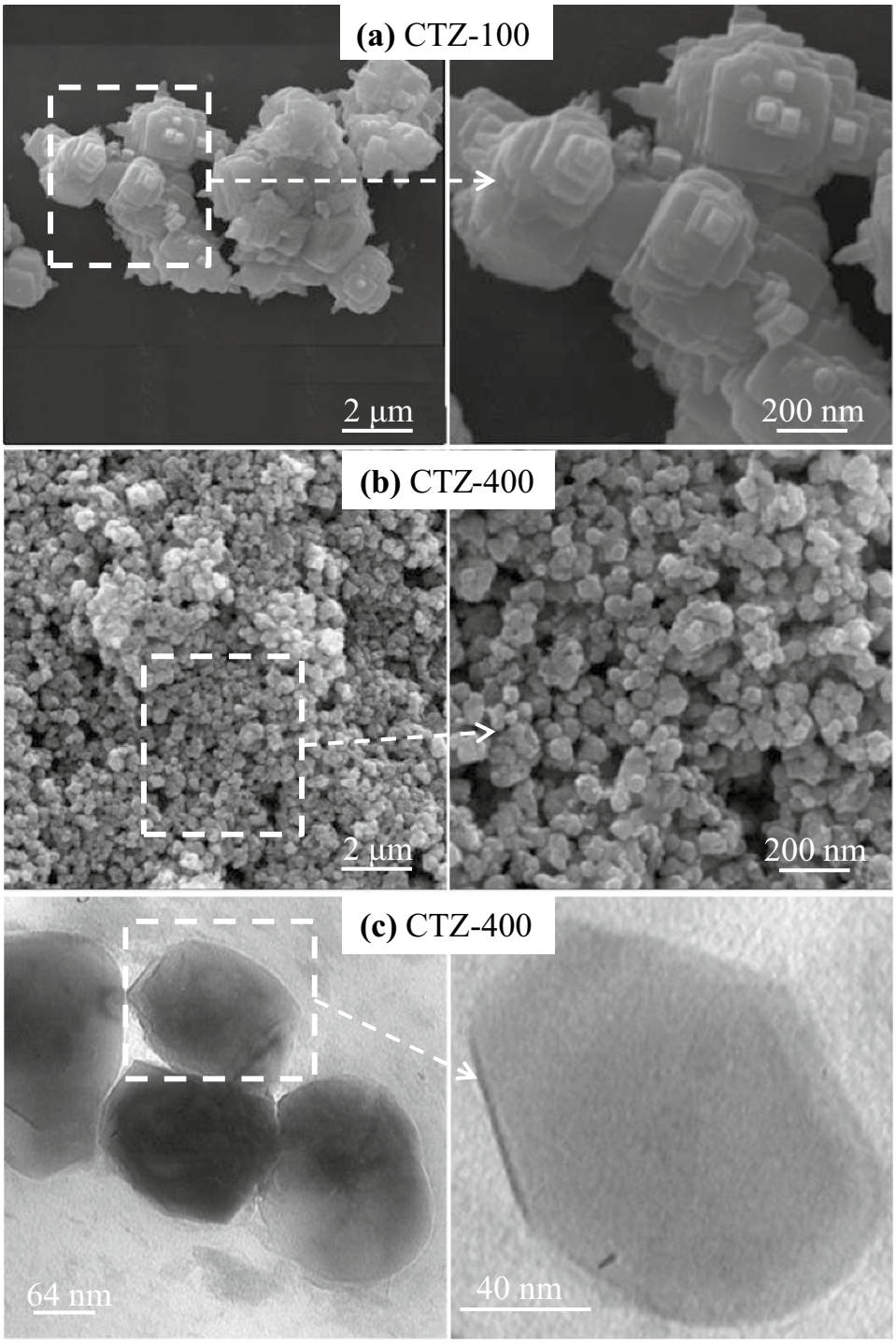

Fig. 5 SEM images of **a** CaO/TiO_2–ZrO_2 calcined at **a** 100 and **b** 400 °C and **c** TEM images of CaO/TiO_2–ZrO_2 calcined 400 °C

reduction of the cost of energy and equipment, 150 °C was selected as the optimum temperature.

Assessing the effect of reaction time showed that the conversion increases quickly within the first 4 h and then remains nearly constant. Thus, 4 h was the suitable reaction time.

Since the esterification reaction is a reversible reaction, a greater methanol/oleic acid molar ratio than stoichiometric molar ratio (3:1) required to shift the equilibrium towards the direction of ester formation. According to Table 2, a 12:1 molar ratio of methanol/oleic acid is quite enough for achieving a good conversion. The conversion decreased by excess methanol over 12 molar ratios of methanol/oleic acid due to occupation of catalyst's pores, decreasing the active sites and deactivation of the catalyst and increasing the separation problem [23, 48].

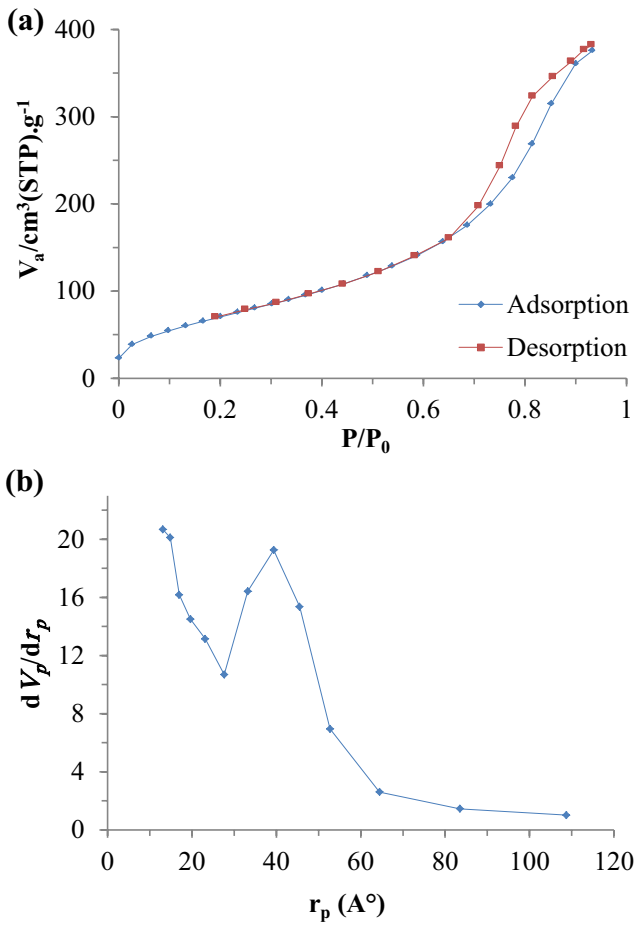

Fig. 6 **a** Hysteresis loop of N_2 adsorption–desorption isotherms and **b** BJH plot of pore size distribution of CTZ-400

Table 2 Optimization of the esterification reaction conditions catalyzed by CaO/ZrO_2–TiO_2 nanocatalysts calcined at 400 °C

Run	Temperature (°C)	Reaction time (h)	Methanol/oleic acid molar ratio	Catalyst amount (wt%)	Conversion (%)
1	90	4	9:1	3	40.3 ± 6.5
2	120	4	9:1	3	62.8 ± 4.7
3	150	4	9:1	3	86.2 ± 4.3
4	180	4	9:1	3	87.5 ± 3.8
5	150	1	9:1	3	23.4 ± 6.3
6	150	2	9:1	3	55.0 ± 4.1
7	150	3	9:1	3	74.7 ± 4.8
8	150	5	9:1	3	86.3 ± 3.4
9	150	4	6:1	3	61.6 ± 5.2
10	150	4	12:1	3	89.5 ± 3.1
11	150	4	15:1	3	75.4 ± 5.2
12	150	4	12:1	1	18.5 ± 2.5
13	150	4	12:1	2	55.9 ± 4.7
14	150	4	12:1	4	90.4 ± 2.8

The effect of catalyst loading on the conversion was evaluated with various catalyst loadings over the range of 1–5 wt%. The conversion increased from 18.5 to 89.5% with an increase in the catalyst loading from 1 to 3 wt%. However, the conversion increased slightly to 90.4% with a further increase which shows using more amount of catalyst does not distinctly change the conversion. Therefore, results revealed that the optimum catalyst loading amount is 3 wt%.

Reusability of CTZ-400 in the esterification reaction under optimum conditions

The reusability of solid catalyst is an important factor to determine its economical application and industrial production of catalyst [49]. In this regard, the catalyst was filtered from the product mixture after each reaction and washed twice with methanol. The recovered catalyst was then dried in oven for overnight and subsequently reused in next run. The results are illustrated in Table 3. The CTZ-400 nanocatalyst preserved its catalytic activity after five runs without any remarkable decrease in the conversion which indicated its excellent property for industrial usage. Increasing the stability of CTZ-400 can be corresponded to Ti cations, which increased the stability of the catalyst as reported by other researchers [19–21].

Conclusions

In this study, the novel sol–gel citrate method was presented for fabrication of CaO/ZrO_2–TiO_2 nanocatalyst. The sample was calcined at different temperatures and its effect was evaluated on the physicochemical properties and catalytic performance in the esterification of oleic acid. The result showed that zirconia had significant effect on the structure of CaO/TiO_2 structure such that the sample was transformed from amorphous structure to crystalline structure. The new phases of $CaZrO_3$ were successfully formed by zirconia loading, which had significant influence on the basicity of sample. Moreover, zirconia increased the acid strength of the CaO/TiO_2 due to its amphoteric properties. Assessment of calcination temperature showed that the highest conversion was obtained with using CTZ-400 nanocatalyst, whereas other samples exhibited a desirable activity to convert greater than 60% of feedstock to ester as compared to CT-400. The

Table 3 Reusability of CaO/TiO_2–ZrO_2 nanocatalysts calcined at 400 °C

Run	First	Second	Third	Forth	Fifth
Conversion (%)	89.5 ± 3.1	88.6 ± 2.8	87.5 ± 3.4	85.7 ± 4.0	84.2 ± 3.7

calcination temperature caused excellent growth of CTZ-400 particles and uniform particles with uniform size were obtained. After choosing the best temperature for calcination of CaO/TiO_2–ZrO_2 nanocatalyst, the esterification reaction conditions using the catalyst were optimized. The optimum reaction conditions were obtained at 150 °C, 12 molar ratio of methanol/oleic acid, 3 wt% of catalyst and 4 h of reaction time. The results of stability of the CTZ-400 showed that the nanocatalyst can preserve its activity at least for five times for several usages that can be refer to presence of titanium cations in the structure of nanocatalyst.

Acknowledgements This work was financially supported by the Ferdowsi University of Mashhad and Iran Nanotechnology Initiative Council (Grant number: 74417).

Open Access This article is distributed under the terms of the Creative Commons Attribution 4.0 International License (http://creativecommons.org/licenses/by/4.0/), which permits unrestricted use, distribution, and reproduction in any medium, provided you give appropriate credit to the original author(s) and the source, provide a link to the Creative Commons license, and indicate if changes were made.

References

1. El Doukkalia, A.I., Arias, P.L., Requies, J., Gandaríasb, I., Jalowiecki-Duhamel, L., Dumeignil, F.: A comparison of sol–gel and impregnated Pt Or/And Ni based γ-alumina catalysts for bioglycerol aqueous phase reforming. Appl. Catal. B **125**, 516–529 (2012)
2. Soltani, S., Rashid, U., Al-Resayes, S.I., Nehdi, I.A.: Recent progress in synthesis and surface functionalization of mesoporous acidic heterogeneous catalysts for esterification of free fatty acid feedstocks: a review. Energy Convers. Manage. **141**, 183–205 (2017)
3. De Lima, A.L., Mota, C.J.A.: Heterogeneous basic catalysts for biodiesel production. Catal. Sci. Technol. **6**, 2877–2891 (2016)
4. Jamil, F., Al-Haj, L., Al-Muhtaseb Ala'a, H., Al-Hinai Mohab, A., Baawain, M., Rashid, U., Ahmad Mohammad, N.M.: current scenario of catalysts for biodiesel production: a critical review. Rev. Chem. Eng. **34**, 267–297 (2018)
5. Tang, Z.E., Lim, S., Pang, Y.L., Ong, H.C., Lee, K.T.: Synthesis of biomass as heterogeneous catalyst for application in biodiesel production: state of the art and fundamental review. Renew. Sustain. Energy Rev. **92**, 235–253 (2018)
6. Saravanan, K., Tyagi, B., Shukla, R.S., Bajaj, H.C.: Esterification of palmitic acid with methanol over template-assisted mesoporous sulfated zirconia solid acid catalyst. Appl. Catal. B **172–173**, 108–115 (2015)
7. Mardhiah, H.H., Ong, H.C., Masjuki, H.H., Lim, S., Lee, H.V.: A review on latest developments and future prospects of heterogeneous catalyst in biodiesel production from non-edible oils. Renew. Sustain. Energy Rev. **67**, 1225–1236 (2017)
8. Mansir, N., Taufiq-Yap, Y.H., Rashid, U., Lokman, I.M.: Investigation of heterogeneous solid acid catalyst performance on low grade feedstocks for biodiesel production: a review. Energy Convers. Manage. **141**, 171–182 (2017)
9. Rahmani Vahid, B., Saghatoleslami, N., Nayebzadeh, H., Toghiani, J.: Effect of alumina loading on the properties and activity of SO_4^{2-}/ZrO_2 for biodiesel production: process optimization via response surface methodology. J. Taiwan Inst. Chem. Eng. **83**, 115–123 (2018)
10. Shim, J.O., Jang, W.J., Jeon, K.W., Lee, D.W., Na, H.S., Kim, H.M., Lee, Y.L., Yoo, S.Y., Jeon, B., Roh, H.S., Ko, C.H.: Petroleum like biodiesel production by catalytic decarboxylation of oleic acid over Pd/Ce-ZrO_2 under solvent-free condition. Appl. Catal. A **563**, 163–169 (2018)
11. Karthikeyan, M., Renganathan, S., Baskar, G.: Production of biodiesel from waste cooking oil using $MgMoO_4$-supported TiO_2 as a heterogeneous catalyst. Energy Sour. A. **39**, 2053–2059 (2017)
12. Kwiatkowski, M., Chassagnon, R., Heintz, O., Geoffroy, N., Skompska, M., Bezverkhyy, I.: Improvement of photocatalytic and photoelectrochemical activity of ZnO/TiO_2 core/shell system through additional calcination: insight into the mechanism. Appl. Catal. B **204**, 200–208 (2017)
13. Marchetti, J.M., Avhad, M.R.: Innovation in solid heterogeneous catalysis for the generation of economically viable and ecofriendly biodiesel: a review. Catal. Rev. Sci. Eng. **58**, 157–208 (2016)
14. Ngamcharussrivichai, P.T., Bunyakiat, K.: Ca and Zn mixed oxide as a heterogeneous base catalyst for transesterification of palm kernel oil. Appl. Catal. A **341**, 77–85 (2008)
15. Zabeti, M., Aroua, M.K.: Biodiesel production using alumina-supported calcium oxide: an optimization study. Fuel Process. Technol. **91**, 243–248 (2010)
16. Ayato, K., Koh, M., Katsuhisa, H.: Development of heterogeneous base catalysts for biodiesel production. Bioresour. Technol. **99**, 3439–3443 (2008)
17. Xia, S., Guo, X., Mao, D., Shi, Z., Wu, G., Lu, G.: Biodiesel synthesis over the CaO–ZrO_2 solid base catalyst prepared by a urea–nitrate combustion method. RSC Adv. **4**, 51688–51695 (2014)
18. Liu, L., Wen, Z., Cui, G.: Preparation of Ca/Zr mixed oxide catalysts through a birch-templating route for the synthesis of biodiesel via transesterification. Fuel **158**, 176–182 (2015)
19. Gardy, J., Hassanpour, A., Lai, X., Ahmed, M.H., Rehan, M.: Biodiesel production from used cooking oil using a novel surface functionalised TiO_2 nano-catalyst. Appl. Catal. B **207**, 297–310 (2017)
20. Gardy, J., Osatiashtiani, A., Céspedes, O., Hassanpour, A., Lai, X., Lee, A.F., Wilson, K., Rehan, M.: A magnetically separable SO_4/Fe-Al-TiO_2 solid acid catalyst for biodiesel production from waste cooking oil. Appl. Catal. B **234**, 268–278 (2018)
21. Kesić, Z., Lukić, I., Zdujić, M., Jovalekić, Č., Veljković, V., Skala, D.: Assessment of $CaTiO_3$, $CaMnO_3$, $CaZrO_3$ and $Ca2Fe_2O_5$ perovskites as heterogeneous base catalysts for biodiesel synthesis. Fuel Process. Technol. **143**, 162–168 (2016)
22. Furuta, S., Matsuhahashi, H., Arata, K.: Biodiesel fuel production with solid amorphous-zirconia catalysis in fixed bed reactor. Biomass Bioenergy **30**, 870–873 (2006)
23. Nayebzadeh, H., Saghatoleslami, N., Tabasizadeh, M.: Application of microwave irradiation for preparation of a KOH/calcium aluminate nanocatalyst and biodiesel. Chem. Eng. Technol. **40**, 1826–1834 (2017)
24. Nayebzadeh, H., Saghatoleslami, N., Maskooki, A., Rahmani Vahid, B.: Effect of calcination temperature on catalytic activity of synthesis SrO/S-ZrO_2 by solvent-free method in esterification of oleic acid. Chem. Biochem. Eng. Q. **27**, 267–273 (2013)
25. Rahmani Vahid, B., Saghatoleslami, N., Nayebzadeh, H., Maskooki, A.: Preparation of nano-size Al-promoted sulfated zirconia and the impact of calcination temperature on its catalytic activity. Chem. Biochem. Eng. Q. **26**, 71–77 (2012)
26. Jeon, K.W., Shim, J.O., Jang, W.J., Lee, D.W., Na, H.S., Kim, H.M., Lee, Y.L., Yoo, S.Y., Roh, H.S., Jeon, B.H., Bae, J.W., Ko, C.H.: Effect of calcination temperature on the association between free NiO species and catalytic activity of Ni–$Ce_{0.6}Zr_{0.4}O_2$

deoxygenation catalysts for biodiesel production. Renew. Energy **131**, 144–151 (2019)
27. Vieira, S.S., Graça, I., Fernandes, A., Lopes, J.M.F.M., Ribeiro, M.F., Magriotis, Z.M.: Influence of calcination temperature on catalytic, acid and textural properties of SO_4^{2-}/La_2O_3/HZSM-5 type catalysts for biodiesel production by esterification. Microporous Mesoporous Mater. **270**, 189–199 (2018)
28. Rahemi, N., Haghighi, M., Babaluo, A., Jafari, M., Allahyari, S.: The effect of the calcination temperature on the physicochemical properties and catalytic activity in the dry reforming of methane over a Ni-Co/Al_2O_3-ZrO_2 nanocatalyst prepared by a hybrid impregnation-plasma method. Catal. Sci. Technol. **3**, 3183–3191 (2013)
29. Nayebzadeh, H., Saghatoleslami, N., Rahmani Vahid, B., Maskooki, A.: Effect of calcination temperature on catalytic activity of synthesis SrO/S-ZrO_2 by solvent-free method in esterification of oleic acid. Chem. Biochem. Eng. Q. **23**, 267–273 (2013)
30. Meng, Y.L., Wang, B.Y., Li, S.F., Tian, S.J., Zhang, M.H.: Effect of calcination temperature on the activity of solid Ca/Al composite oxide-based alkaline catalyst for biodiesel production. Bioresour. Technol. **128**, 305–309 (2013)
31. Faycal Atitar, M., Ismail, A.A., Al-Sayari, S.A., Bahnemann, D., Afanasev, D., Emeline, A.V.: Mesoporous TiO_2 nanocrystals as efficient photocatalysts: impact of calcination temperature and phase transformation on photocatalytic performance. Chem. Eng. J. **264**, 417–424 (2015)
32. Li, M., Li, X., Jiang, G., He, G.: Hierarchically macro–mesoporous ZrO_2–TiO_2 composites with enhanced photocatalytic activity. Ceram. Int. **41**, 5749–5757 (2015)
33. Reddy, B.M., Reddy, G.K., Rao, K.N., Katta, L.: Influence of alumina and titanium on the structure and catalytic properties of sulfated zirconia: Beckmann rearrangement. J. Mol Catal. A. **306**, 62–68 (2009)
34. Wang, H., He, L., Liu, Z.: Supporting tungsten oxide on zirconia by hydrothermal and impregnation methods and its use as a catalyst to reduce the viscosity of heavy crude oil. Energy Fuel. **26**, 6518–6527 (2012)
35. Chen, J., Cai, Z., Chen, X., Zheng, X., Zheng, Y.: Facile synthesis of ordered mesoporous CaO-ZrO_2 composite with mild conditions. Mater. Lett. **168**, 214–217 (2016)
36. Mongkolbovornkij, V.C., Sutthisripok, W., Laosiripojana, N.: Esterification of industrial-grade palm fatty acid distillate over modified ZrO_2 (with WO_3–, SO_4– and TiO_2–): effects of co-solvent adding and water removal. Fuel Process. Technol. **91**, 1510–1516 (2010)
37. Yurdakoc, M., Akcay, M., Tonbul, Y., Yurdakoc, K.: Acidity of silica-alumina catalysts by amine titration using Hammett indicators and FT-IR study of pyridine adsorption. Turk. J. Chem. **23**, 319–328 (1999)
38. Tao, G., Hua, Z., Gao, Z., Chen, Y., Wang, L., He, Q., Chen, H., Shi, J.: Synthesis and catalytic activity of mesostructured KF/$CaxAl_2O_{(x+3)}$ for the transesterification reaction to produce biodiesel. RSC Adv. **2**, 12337–12345 (2012)
39. Li, W., Deng, Q., Fang, G., Chen, Y., Zhan, J., Wang, S.: Facile synthesis of Fe_3O_4@TiO_2-ZrO_2 and its application in phosphopeptide enrichment. J. Mater. Chem. B. **1**, 1947–1961 (2013)
40. Hojjat, M., Nayebzadeh, H., Khadangi-Mahrood, M., Rahmani-Vahid, B.: Optimization of process conditions for biodiesel production over CaO–Al_2O_3/ZrO_2 catalyst using response surface methodology. Chem. Pap. **71**, 689–698 (2016)
41. Nayebzadeh, H., Saghatoleslami, N., Maskooki, A., Rahmani Vahid, B.: Preparation of supported nanosized sulfated zirconia by strontia and assessment of its activities in the esterification of oleic acid. Chem. Biochem. Eng. Q. **25**, 259–265 (2014)
42. Xie, Y.L., Chun, H.: Biodiesel preparation from soybean oil by using a heterogeneous $Ca_xMg_{22-x}O_2$ catalyst. Catal. Lett. **142**, 352–359 (2012)
43. Nayebzadeh, H., Haghighi, M., Saghatoleslami, N., Tabasizadeh, M., Yousefi, S.: Fabrication of carbonated alumina doped by calcium oxide via microwave combustion method used as nanocatalyst in biodiesel production: influence of carbon source type. Energy Convers. Manage. **171**, 566–575 (2018)
44. Rahemi, N., Haghighi, M., Babaluo, A., Jafari, M., Khorram, S.: Non-thermal plasma assisted synthesis and physicochemical characterizations of Co and Cu doped Ni/Al_2O_3 nanocatalysts used for dry reforming of methane. Int. J. Hydrogen Energy **38**, 16048–16061 (2013)
45. Laha, S.C., Mukherjee, P., Sainkar, S.R., Kumar, R.: Cerium containing MCM-41-type mesoporous materials and their acidic and redox catalytic properties. J. Catal. **207**, 213–223 (2002)
46. Rahmani Vahid, B., Haghighi, M.: Biodiesel production from sunflower oil over MgO/$MgAl_2O_4$ nanocatalyst: effect of fuel type on catalyst nanostructure and performance. Energy Convers. Manage. **134**, 290–300 (2017)
47. Ramesh, B.S., Bhat, Y.S.: Enhancing Brønsted acid site activity of ion exchanged montmorillonite by microwave irradiation for ester synthesis. Appl. Clay Sci. **48**, 159–163 (2010)
48. Nayebzadeh, H., Saghatoleslami, N., Haghighi, M., Tabasizadeh, M., Binaeian, E.: Comparative assessment of the ability of a microwave absorber nanocatalyst in the microwave-assisted biodiesel production process. Compt. Rend. Chim. **21**, 676–683 (2018)
49. Hashemzehi, M., Saghatoleslami, N., Nayebzadeh, H.: A study on the structure and catalytic performance of $Zn_xCu_{1-x}Al_2O_4$ catalysts synthesized by the solution combustion method for the esterification reaction. Compt. Rend. Chim. **19**, 955–962 (2016)

Publisher's Note Springer Nature remains neutral with regard to jurisdictional claims in published maps and institutional affiliations.

Affiliations

Aliakbar Sistani[1] · Naser Saghatoleslami[1,2] · Hamed Nayebzadeh[1]

✉ Hamed Nayebzadeh
h.nayebzadeh@yahoo.com;
hamed.nayebzadeh@mail.um.ac.ir

[1] Department of Chemical Engineering, Faculty of Engineering, Ferdowsi University of Mashhad, P.O.Box 9177948974, Mashhad, Iran

[2] Department of Petroleum Engineering, Eqbal Institute of Higher Education, P.O.Box 110623, Mashhad, Iran